Computational Design of Enhanced Learning Protocols

Yili Zhang, Rong-Yu Liu, George A. Heberton,
Paul Smolen, Douglas A. Baxter, Leonard J. Cleary & John H. Byrne

ONLINE METHODS

Model Development. The mathematical model for the activation of PKA and ERK (**Fig. 1a**) was modified from an earlier model by Pettigrew *et al.*[38] of the signaling cascades underlying LTF by only considering the initial (protein-synthesis independent) steps in the induction of LTF. In addition, a time delay was added to the phosphorylation of Raf (see below) and the variable *inducer* was added.

PKA exists largely as an inactive holoenzyme (PKA_{RC}) that consists of regulatory (PKA_R) and catalytic (PKA_C) subunits (**Fig. 1a**). In response to 5-HT treatment, [cAMP] increases, and cAMP binds to the regulatory subunit, leading to the release of active catalytic subunit. The basal level of 5-HT was 0 μM, and during a pulse of 5-HT, its concentration was transiently increased to 50 μM. The dynamics of cAMP following 5-HT treatment and the cAMP-dependent activation of PKA are described by Eqs. 1-4.

$$\frac{d[cAMP]}{dt} = \lambda \frac{[5\text{-}HT]}{[5\text{-}HT] + K_{5HT}} - k_{b,cAMP}[cAMP] \qquad \text{(Eq. 1)}$$

$$\frac{d[PKA_{RC}]}{dt} = k_{b,PKA}[PKA_C][PKA_R] - k_{f,PKA}[PKA_{RC}][cAMP]^2 \qquad \text{(Eq. 2)}$$

$$\frac{d[PKA_R]}{dt} = k_{f,PKA}[PKA_{RC}][cAMP]^2 - k_{b,PKA}[PKA_C][PKA_R] \qquad \text{(Eq. 3)}$$

$$\frac{d[PKA_C]}{dt} = k_{f,PKA}[PKA_{RC}][cAMP]^2 - k_{b,PKA}[PKA_C][PKA_R] \qquad \text{(Eq. 4)}$$

A particle swarm optimization algorithm (PSO)[39] was used to identify the values for model parameters that produced the best fit between model simulations and the time course of short-term PKA activation after 5-HT treatment[13]. The resulting standard parameter values for the PKA pathway were:

λ = 3.64 μM/min, K_{5HT} = 85 μM, $k_{b,cAMP}$ = 1 min^{-1},

$k_{f,PKA}$ = 20 μM^{-2}min^{-1}, $k_{b,PKA}$ = 12 μM^{-1}min^{-1}

The activation of ERK was modeled as a cascade with sequential activation of the kinases Raf, MEK, and ERK (**Fig. 1a**). The differential equations describing the activation of Raf, MEK, and ERK (Eqs. 5-12) are similar to those in Pettigrew *et al.*[38]. However, a discrete time delay (τ_{delay} = 25 min) was added to the phosphorylation of Raf (Eq. 5), to ensure that the transient activation curve of ERK had a narrow peak at ~45 min from the beginning of the first 5-HT pulse[7]. The total amounts of Raf, MEK, and ERK were conserved (Eqs. 6, 9, 12).

$$\frac{d[Raf^{p}]}{dt} = k_{f,Raf}[Raf]\left\langle [5\text{-}HT] \right\rangle_{\tau_{delay}} - k_{b,Raf}[Raf^{p}] \qquad \text{(Eq. 5)}$$

$$[Raf] = [Raf]_{total} - [Raf^{p}] \qquad \text{(Eq. 6)}$$

$$\frac{d[MEK]}{dt} = \frac{k_{b,MEK}[MEK^{p}]}{[MEK^{p}] + K_{MEK,2}} - \frac{k_{f,MEK}[Raf^{p}][MEK]}{[MEK] + K_{MEK,1}} \qquad \text{(Eq. 7)}$$

$$\frac{d[MEK^{pp}]}{dt} = \frac{k_{f,MEK}[Raf^{p}][MEK^{p}]}{[MEK^{p}] + K_{MEK,1}} - \frac{k_{b,MEK}[MEK^{pp}]}{[MEK^{pp}] + K_{MEK,2}} \qquad \text{(Eq. 8)}$$

$$[MEK^{p}] = [MEK]_{total} - [MEK] - [MEK^{pp}] \qquad \text{(Eq. 9)}$$

$$\frac{d[ERK]}{dt} = \frac{k_{b,ERK}[ERK^{p}]}{[ERK^{p}] + K_{ERK,2}} - \frac{k_{f,ERK}[MEK^{pp}][ERK]}{[ERK] + K_{ERK,1}} \qquad \text{(Eq. 10)}$$

$$\frac{d[ERK^{pp}]}{dt} = \frac{k_{f,ERK}[MEK^{pp}][ERK^{p}]}{[ERK^{p}] + K_{ERK,1}} - \frac{k_{b,ERK}[ERK^{pp}]}{[ERK^{pp}] + K_{ERK,2}} \qquad \text{(Eq. 11)}$$

$$[ERK^{p}] = [ERK]_{total} - [ERK] - [ERK^{pp}] \quad \text{(Eq. 12)}$$

The particle swarm optimization (PSO) algorithm was used to identify parameter values that produced a transient phase of ERK activation that fit the time course of transient activation of ERK following tail shock[7]. The standard parameter values for the ERK pathway were:

$k_{f,Raf}$ = 0.004 μM^{-1}min^{-1}, $k_{b,Raf}$ = 0.1 min^{-1}, $[Raf]_{total}$ = 0.5 μM,

$k_{f,MEK}$ = 0.41 min^{-1}, $k_{b,MEK}$ = 0.04 μM/min, $K_{MEK,1}$ = 0.20 μM,

$K_{MEK,2}$ = 0.19 μM, $[MEK]_{total}$ = 0.5 μM, $k_{f,ERK}$ = 0.41 min^{-1},

$k_{b,ERK}$ = 0.12 μM/min, $K_{ERK,1}$ = 0.19 μM,

$K_{ERK,2}$ = 0.21 μM, $[ERK]_{total}$ = 0.5 μM.

The variable '*inducer*' was used to quantify the amount of overlap between PKA and ERK activities. *Inducer* was an abstract representation of the synergistic interaction between PKA- and ERK-dependent regulation of gene expression that is necessary for the induction of LTF. Thus, *inducer* was proportional to the product of PKA and ERK activities (Eq. 13).

$$inducer = k_{inducer}\,[PKA_C]\,[ERK^{pp}] \quad \text{(Eq. 13)}$$

where $k_{inducer}$ = 1 μM^{-1}.

The model was tested initially with a single 5-min pulse of 5-HT to confirm that such a stimulus elicited a transient activation of PKA and delayed, transient activation of ERK with little overlap and therefore little increase in *inducer* (not shown). Similarly, little overlap was produced when two 5-min pulses of 5-HT were applied with an interstimulus interval (ISI, onset to onset) of 15 or 60 min (not shown). A substantial overlap of PKA and ERK activity occurred with an ISI of 45 min (not shown). Substantial overlap (**Fig. 1b**) was also produced by the standard 5-pulse 5-HT protocol that is commonly used empirically to induce LTF (i.e., 5-pulse 5-min 5-HT treatment with uniform 20-min intervals between the start of the pulses)[23,40,41]. To determine whether other protocols could more effectively activate *inducer,* 9,999 alternative protocols were

simulated. Each protocol included five, 5-min 5-HT stimuli, but the ISIs were chosen as multiples of 5 min, in the range from 5-50 min. Thus, each of the four ISIs had 10 possible values (i.e., 10^4 total possible permutations, one of which represented the Standard protocol; **Supplementary Movie 1**).

The synergistic effect of PKA and ERK on the downstream cascades is likely to be nonlinear in that multiple genes necessary for LTF are activated following phosphorylation of transcription factors by PKA and ERK. Such nonlinearity commonly expresses itself as a steep, sigmoidal stimulus-response curve. Therefore, the induction of LTF may be particularly sensitive to the peak levels of PKA and ERK activities, as opposed to a time integral of PKA and/or ERK activities. In view of these considerations, the peak level of *inducer* was used to predict the efficacy of a stimulus protocol. A histogram was constructed to summarize the distribution of peak levels of *inducer* from the above 10^4 protocols. Considerable variability in the peak levels of *inducer* was observed (**Supplementary Fig. 1**). The protocol that maximized the peak was denoted the 'Enhanced' protocol. We predicted that this protocol would enhance LTF.

Although optimization algorithms are available, several factors indicated that optimization algorithms were not necessary in the present study. First, only four parameters were varied in the present study. These four parameters were the interstimulus intervals (ISIs) between the five pulses of 5-HT (see **Supplementary Movie 1**). Given this small number of free parameters, it is likely that our systematic search of the parameter space was sufficient. Second, our search of the ISI-parameter space did not reveal sudden, large changes in simulated protocol efficacies. Rather, peak levels of *inducer* varied smoothly as ISI lengths were varied over the range sampled in the present study (data not shown). Therefore, it is unlikely that further refinement of the search would yield substantially better training protocols. Third, empirical considerations limit the temporal precision with which drugs can be applied and washed out. Thus, ISIs were limited to 5-min increments. For the present study, there was no additional benefit in examining finer increments that could not be experimentally tested. Finally, in this initial study, we were more concerned with

demonstrating the feasibility of predicting training protocols that enhance memory than finding an exact optimum.

Simulations indicated that a protocol that enhanced LTS and LTF would need to satisfy two criteria: 1) significant activation of PKA and ERK, and 2) maximum overlap of these activities. The Enhanced protocol was superior to the Standard protocol because it induced a greater level of ERK and because the peak level of PKA activation induced by the 5^{th} stimulus significantly overlapped with the peak level of ERK activation (compare panels b and c in **Fig. 1**), thus maximizing the level of *inducer*.

Fourth-order Runge-Kutta integration was used for integration of differential equations with a time step of 3 s. No significant improvement in accuracy was found by further time step reduction. The steady-state levels of variables were determined after at least two simulated days, prior to any stimuli. The model was programmed in XPP[42], and simulated on Pentium® III microcomputers. Source codes are available upon request.

Cell culture, 5-HT treatment and electrophysiology. For cellular experiments, *Aplysia californica* were obtained from the NIH-*Aplysia* resource facility, University of Miami, Miami, FL. Motor neurons (MNs) were isolated from abdominal ganglia from juvenile animals (0.8–1.5 gm), and sensory neurons (SNs) were isolated from pleural ganglia from 60–100 gm animals. Isolated SNs or SN-MN co-cultures were prepared according to conventional procedures[43,44]. Dishes of SN cultures were plated with 5-10 SNs. Dishes of SN-MN co-cultures were plated with a single SN and a single L7 MN. Both SN cultures and SN-MN co-cultures were allowed to grow for 5 d at 18°C, and the growth medium was replaced prior to treatments and recordings with a solution of 50% L15 and 50% artificial seawater (ASW; 450 mM NaCl, 10 mM KCl, 11 mM $CaCl_2$, 29 mM $MgCl_2$, 10 mM HEPES at pH 7.6). Long-term facilitation (LTF) was induced by repeated 5-HT treatment. Five, 5-min pulses of either vehicle (L15:ASW) or 50 μM 5-HT (Sigma, St Louis, MO) were applied to the bath with ISIs as described in the Results (see **Fig. 1b,c**).

Stimulation of presynaptic SNs was performed extracellularly using a blunt patch electrode filled with L15:ASW. Intracellular recordings from MNs were made with 10-20

MΩ sharp electrodes filled with 3 M potassium acetate connected to an Axoclamp 2-B amplifier (Molecular Devices, Sunnyvale, CA)[41]. Data acquisition and analyses of resting potential, input resistance, and amplitude of excitatory postsynaptic potentials (EPSPs) were performed with pCLAMP 8 software (Molecular Devices, Sunnyvale, CA). MNs were current clamped at −90 mV before measurement of EPSPs. Pre-treatment measurements of EPSP amplitudes varied from 5 to 45 mV. Cultures were excluded from further use if EPSPs were less than 5 mV or sufficiently large to trigger an action potential. MNs that had initial resting potentials more positive than –30 mV or input resistances less than 10 MΩ were also excluded from the analyses. Immediately after the end of treatment with 5-HT, cultures were returned to culture medium. At 1 d, 2 d, and 5 d after treatment, EPSP amplitudes were assessed in the same manner as the baseline measurements. In cases where the post-test EPSP amplitude was accompanied by an action potential, the EPSP amplitude was assigned a value of 45 mV because the largest synaptic potential obtained in our culture system never exceeded that amplitude. Statistical analyses (one-way ANOVA) indicated that the pretest scores for each group were not significantly different ($F_{2,26}$ = 0.25). Thus, for statistical analysis, the amplitudes of the EPSPs at 1, 2, and 5 days after treatment were normalized to the EPSPs measured before treatment (i.e., post/pre).

CREB1 phosphorylation. For immunofluorescence analysis, SN *c*ultures were treated with five, 5 min pulses of 50 μM 5-HT. The intervals between the start of the 5-HT pulses (i.e., the ISIs) were either 20 min (Standard protocol, see **Fig. 1b**) or 10, 10, 5, and 30 min (Enhanced protocol, see **Fig. 1c**). A separate group of control cultures were not treated with 5-HT, but were treated with vehicle alone (L15:ASW) with an ISI of 20 min. Immediately or 18 h after the end of treatment, cells were fixed in a solution of 4% paraformaldehyde in PBS containing 30% sucrose and blocked for 30 min at room temperature in Superblock blocking buffer (Pierce, Holmdel, NJ)/0.2% Triton X-100/3% normal goat serum. Subsequently, fixed cells were incubated overnight at 4°C with anti-pCREB1 antibody (1:500), which specifically recognizes the phosphorylated form of *Aplysia* CREB1 protein[45], followed by secondary antibody (goat anti-rabbit IgG conjugated to Cy-3; 1:200 dilution; Jackson ImmunoResearch, West Grove, PA) incubation for 1 h at room temperature. Images were obtained with a Zeiss LSM510

confocal microscope using a 63X oil immersion lens. A z-series of optical sections through the cell body (0.5 μm increments) was taken, and the section through the middle of the nucleus was used for analysis of mean nuclear fluorescence intensity with the MetaMorph Offline software (Universal Imaging Corporation, West Chester, PA). Five to 10 neurons on each coverslip were analyzed, and measurements from neurons on the same coverslip were averaged. The levels of phosphorylated CREB1 in the Standard and Enhanced groups were normalized to the vehicle controls (**Fig. 3b**). The number of samples (n) reported in the text indicates the number of dishes. This experiment was done in a "blind" manner because different investigators carried out 5-HT treatments and immunofluorescence staining/image analysis.

Behavioral training. *Aplysia californica* (100–150 gm) were obtained from Alacrity Marine Biological (Redondo Beach, CA) and Marinus Inc. (Long Beach, CA). Animals were prepared for long-term sensitization training as described previously[9]. Test stimuli were delivered through a pair of silver-wire electrodes implanted in each side of the tail, and siphon withdrawals were elicited by a brief electrical stimulus delivered to the tail. Prior to testing, a stimulus threshold (i.e., the minimum amount of stimulating current necessary to elicit a withdrawal response) was determined for each side (contra- and ipsilateral to the training site; see below) of each animal (animals in the Standard and Enhanced groups). Statistical analyses (one-way ANOVA) indicated that the intensities of the threshold stimuli were not significantly different among the four measurements ($F_{3,56}$ = 0.46). The overall average for the threshold stimulus was 1.97 ± 0.13 mA (mean ± s.e.m.). The intensity of subsequent test stimuli was set to 170% of the previously determined threshold for each side of each animal. Following a pre-training assessment of the strength of the reflex elicited by stimuli to the left and right side of the animal, five trains (1 Hz, 10 s) of sensitizing stimuli were delivered at the same intertrial intervals (ITIs) as used for the electrophysiological experiments on LTF. Sensitizing stimuli were applied to the lateral body wall of one randomly chosen side of the animal via a hand-held electrode. The left side was used for training in roughly the same number of experiments as the right. Because sensitization is lateralized[9], the contralateral side of each animal was used as a control. The post-training assessment was performed 1 d and 5 d after training. The duration of siphon withdrawal was

measured in response to each of five test stimuli. Data were excluded if the animals failed to respond to at least three of the five test stimuli because failed responses suggested nonfunctioning stimulating electrodes. Average responses before and after training were calculated, and the averaged response durations 1 d and 5 d after training were expressed as the ratio 'post/pre' (see **Fig. 4**). Statistical analyses (one-way ANOVA) indicated that the ipsi- and contralateral pretest responses for each group were not significantly different ($F_{3,50}$ = 0.14). The average pretest responses (mean ± s.e.m.) for the contra- and ipsilateral sides in the Standard group were 4.4 ± 0.9 s and 3.9 ± 0.6 s, respectively. The average pretest responses for the contra- and ipsilateral sides in the Enhanced group were 3.8 ± 0.6 s and 3.9 ± 0.5 s, respectively. Statistical analyses (two-sample t test) also indicated that the post-test contralateral responses (i.e., control responses) were not significantly different between the Standard and Enhanced groups one day after training ($t_{2,20}$ = 1.32) or five days after training ($t_{2,14}$ = 0.01). Therefore the contralateral responses for the Standard and Enhanced groups were combined into one Control group for 1 d and another Control group for 5 d after training (**Fig. 4**, black bars). In all experiments, different investigators carried out testing and training, and the investigator testing the animals was unaware of their prior treatment. All behavioral experiments were conducted at 15° C.

Statistical analysis. All statistical analyses were performed using SigmaPlot (version 11) software (Systat Software, Inc., San Jose, CA). The specific types of statistical tests, the n for each analysis, P values, and other relevant statistical values (e.g., means, s.e.m., F, q, and t values) are given at the appropriate places throughout the text.

SUPPLEMENTARY INFORMATION

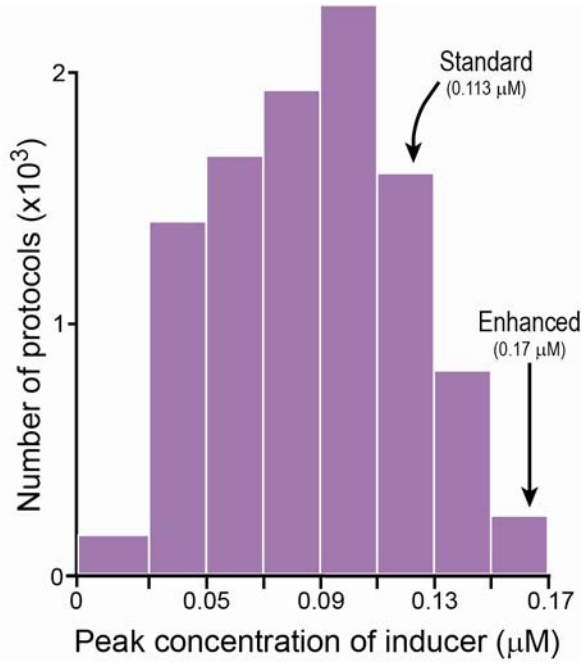

Supplementary Figure 1 Histogram of peak levels of *inducer* from 10^4 protocols. The range of peak levels of *inducer* (0 - 0.17 μM) was subdivided into 8 bins, and the number of simulations that produced a peak concentration of *inducer* in each subdivision was plotted. The arrows indicate which bins contained the peak concentrations of *inducer* for the Standard and Enhanced protocols (see **Fig. 1b,c**).

Supplementary Movie 1 Schematic represent of algorithm used to generate training protocols. The QuickTime movie illustrates how 10,000 different protocols were generated by systematically varying ISIs between 5-HT pulses. Protocols are numbered from 1 to 10,000. Protocol 1 is a massed protocol (i.e., 25 min continuous 5-HT application), whereas Protocol 10,000 has uniform 50-min intervals between the start of the pulses.